Softening Caused by Profuse Shear Banding in a Bulk Metallic Glass

H. Bei,[1,2] S. Xie,[1] and E. P. George[1,2]

[1]*Department of Materials Science and Engineering, The University of Tennessee, Knoxville, Tennessee 37996, USA*
[2]*Metals and Ceramics Division, Oak Ridge National Laboratory, Oak Ridge, Tennessee 37831, USA*

(Received 29 November 2005; published 16 March 2006)

By controlling the specimen aspect ratio and strain rate, compressive strains as high as 80% were obtained in an otherwise brittle metallic glass. Physical and mechanical properties were measured after deformation, and a systematic strain-induced softening was observed which contrasts sharply with the hardening typically observed in crystalline metals. If the deformed glass is treated as a composite of hard amorphous grains surrounded by soft shear-band boundaries, analogous to nanocrystalline materials that exhibit inverse Hall-Petch behavior, the correct functional form for the dependence of hardness on shear-band spacing is obtained. Deformation-induced softening leads naturally to shear localization and brittle fracture.

DOI: 10.1103/PhysRevLett.96.105503 PACS numbers: 81.05.Kf, 62.20.Fe, 81.40.Ef, 81.70.Bt

Metallic glasses have many attractive properties including high strength, elastic deformability, and corrosion resistance (e.g., [1–5]). The recent discovery that some of these glasses can be produced in bulk form has renewed interest in their mechanical behavior. A major drawback of bulk metallic glasses (BMGs) is their brittleness at temperatures significantly below the glass transition temperature (T_g), which has hampered our ability to cold work these materials, understand their mechanisms of plastic deformation, and investigate how structure and properties change with strain.

Plastic deformation in crystalline metals occurs by the motion and multiplication of lattice defects called dislocations (e.g., [6]). Amorphous metals, in contrast, lack long-range order; therefore, dislocation-mediated plasticity is not possible in these materials. Nanoindentation has shown that plasticity begins to occur in BMGs at shear stresses of $\sim G/10$ [7], where G is the shear modulus, consistent with the notion that, in the absence of dislocations, yielding can occur only at stresses approaching the theoretical strength.

Although their detailed mechanisms of plastic deformation are not well understood, it is known that, after an initial elastic range, BMGs deform by highly localized shear (e.g., [8–13]). Unlike in crystalline metals, where dislocation interactions produce strain hardening and homogeneous deformation [6], once plasticity is initiated in a metallic glass, it remains localized in narrow zones called shear bands and does not spread through the material. As a result of this inhomogeneous deformation, specimens shear off at $\sim 45°$ to the loading axis in a macroscopically brittle manner with plastic strains $<2\%$ [8,9], except in a few cases [10,14].

The cause of this shear localization is not clear, but it may be because metallic glasses, unlike their crystalline counterparts, do not harden when plastically deformed. Unfortunately, it is not easy to verify this, because it is difficult to measure hardness directly on narrow shear bands (even by nanoindentation). Furthermore, to make accurate measurements, the surface steps associated with shear bands have to be removed by polishing to create a flat surface. Once that is done, the shear bands are erased, and it becomes difficult to determine the location of a hardness indent relative to a shear band. To our knowledge, there are only three papers in the literature dealing with deformation-induced softening of metallic glasses. The first is a review paper by Masumoto and Maddin [15], where unpublished results of Masumoto and Koiwa are reported that show a decrease in the hardness of an amorphous $Pd_{80}Si_{20}$ ribbon after 40% reduction in thickness by cold rolling. The next is a paper by Tang, Li, and Zeng [16], in which the hardness of a Zr-based BMG was measured by nanoindentation after it had been indented with a 200 μm sphere. Hardness was reported to be lower near the spherical indent, where shear bands were present, than far away in the undeformed glass. However, since the surface was not polished after spherical indentation, the subsequent nanoindentation measurements may have been influenced by the presence of surface steps at shear bands. The last paper is that of Jiang, Pinkerton, and Atzmon [17], who showed that the hardness of a 22 μm-thick Al-Ni-Y amorphous ribbon decreased from 3.89 to 3.48 GPa after cold rolling reduced its thickness by 45.5%.

Given the paucity of experimental data, we set out to systematically investigate how the hardness of a BMG changes as a function of applied plastic strain and correlate the results with changes in shear-band density. A Zr-based BMG, $Zr_{52.5}Cu_{17.9}Ni_{14.6}Al_{10}Ti_5$, was chosen for this study because of its good glass formability, which allowed amorphous castings 6.7 mm in diameter to be easily produced [9]. Our results show that, if the specimen aspect ratio (A = height/diameter) and strain rate ($\dot{\varepsilon}$) are carefully controlled, a BMG can be uniaxially compressed by as much as 80%, which is much higher than anything previously reported. Physical and mechanical properties were then measured as a function of plastic strain.

Figure 1(a) shows cylindrical specimens having an initial height and aspect ratio of 3.5 mm and 0.52, respectively, after various amounts of compression at an

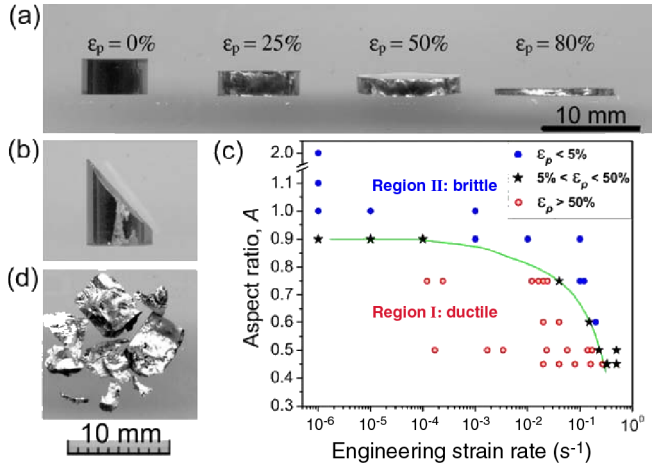

FIG. 1 (color online). Room-temperature compression of a Zr-based metallic glass with $T_g = 390\,^{\circ}\mathrm{C}$. (a) Change in height of low-aspect-ratio specimens after plastic straining. (b) High-aspect-ratio specimen exhibiting brittle fracture at ~45° to the vertical loading axis. (c) "Deformation map" showing the effects of aspect ratio and strain rate on the plastic strain to failure. (d) At high strain rates, brittle fracture occurs even in low-aspect-ratio specimens.

engineering strain rate of $1.7 \times 10^{-3}\ \mathrm{s}^{-1}$. The compressed specimens were metallographically polished and examined in a scanning electron microscope. No microcracks were observed anywhere on the polished surface. Clearly, by geometrically constraining the shear bands ($A < 1$), extensive plastic deformation of the BMG is possible even at room temperature, which is a low temperature compared to its T_g of ~390 °C. The plastic strain (ε_p) achievable is 80%, which is significantly higher than anything previously reported in relatively thick specimens of single-phase BMGs. X-ray diffraction revealed no evidence of crystallization, even in our most heavily deformed specimens.

When A is increased to 2, i.e., the physical constraint on the shear bands is removed, the BMG fractures in a brittle manner ($\varepsilon_p < 1.0\%$) at ~45° to the loading axis [Fig. 1(b)], consistent with other reports (e.g., [9]). Interestingly, at high strain rates (e.g., $>5 \times 10^{-1}\ \mathrm{s}^{-1}$), brittle fracture occurs regardless of the aspect ratio. Both parameters are therefore important in determining whether extensive plastic deformation is possible. Large strains have been obtained by us also in Cu-based BMGs ($Cu_{60}Zr_{10}Hf_{15}Ti_{15}$ and $Cu_{60}Zr_{30}Ti_{10}$), indicating that this approach is not limited to just one glass composition.

Figure 1(c) is a "deformation map" for the Zr-based BMG showing the combined effects of aspect ratio and strain rate on plastic strain. There are two distinct regions: Region I, where aspect ratio and strain rate are low, is the ductile region; here extensive plastic deformation ($\varepsilon_p > 50\%$) is possible without specimen fracture. Region II, with high aspect ratio and/or strain rate, is the brittle region ($\varepsilon_p < 5\%$). Previous compression tests on single-phase BMGs (e.g., [8,9]) generally fall within this second region.

The above results may be rationalized as follows. When the aspect ratio is greater than 1, the specimens shear off at ~45° to the loading axis [Fig. 1(b)] as a result of a few highly localized shear bands propagating unrestricted through the specimen. In contrast, when $A < 1$, the compression platens block the 45° shear bands from going through the sample, thereby forcing the nucleation of new shear bands to carry the plastic deformation. The resulting multiplication of shear bands redistributes plastic strain and helps prevent crack formation. The effect of the second parameter, strain rate, on plastic strain is the result of competition between stress buildup and relaxation. At low strain rates, there is enough time for the blocked shear bands to release the built-up stresses and avoid crack formation. At high strain rates, the tensile components of the built-up stresses do not have enough time to relax, which leads to brittle fracture and sometimes even shattering of the specimens [Fig. 1(d)]. This is the first time that a strain rate effect on deformability has been reported in a BMG strained at a temperature significantly below T_g; usually, strain rate effects are observed only at temperatures close to T_g where BMGs exhibit viscous flow [18–20].

Macroscopically, the glass deforms homogenously, i.e., decreases in thickness uniformly. Microscopically, the mode of plastic deformation is inhomogeneous flow with multiple shear bands forming on the specimen surfaces. Figure 2(a) shows the shear bands visible on a free surface parallel to the loading direction. Since the shear bands are distributed over the entire surface in a grid pattern, we measured their linear density as a function of the overall plastic strain. The results, Fig. 2(b), show a linear increase (decrease) in the density (spacing) of shear bands with increasing strain:

$$\rho = 0.14\varepsilon_P, \qquad d^{-1} = 0.14\varepsilon_P, \tag{1}$$

where ρ is the shear-band density (units of $\mu\mathrm{m}^{-1}$), d is the shear-band spacing ($d = \rho^{-1}$), and ε_p is the plastic strain. From these results, the average displacement per shear band is calculated to be ~7 μm, which is comparable to the average shear offsets (~5 μm) produced at the intersections of shear bands [arrows in Fig. 2(a)].

Figure 3 shows that the hardness decreases linearly with increasing plastic strain and decreasing shear-band spacing. These hardness values (nanoindentation as well as the two sets of Vickers data obtained at different loads) reflect the composite properties of the shear bands plus the surrounding undeformed glass. This is because our hardness impressions vary in size from 2–30 μm, whereas the shear-band spacing varies from 10–100 μm. As mentioned earlier, it is very difficult to measure the hardness of just the shear bands.

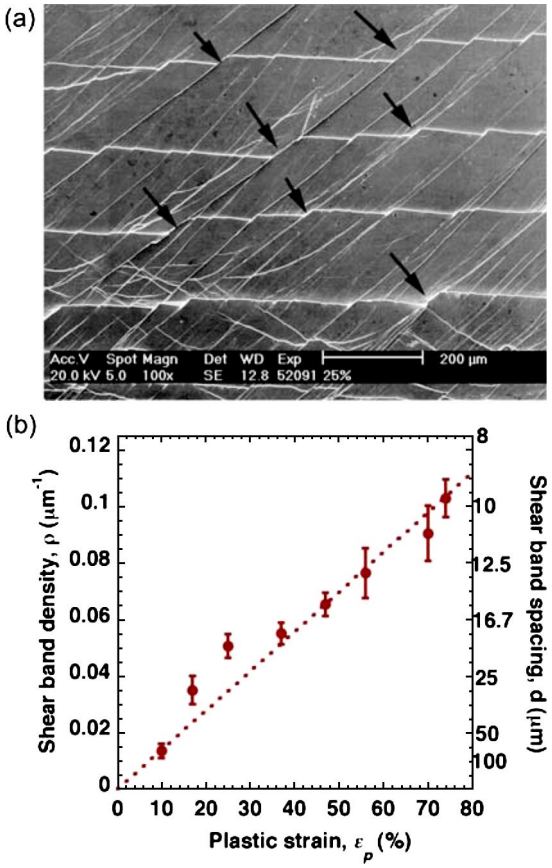

FIG. 2 (color online). (a) Profuse shear banding visible on a free surface parallel to the compression direction (which is vertical here); arrows point to offsets at shear-band intersections. (b) Linear increase (decrease) in the shear-band density (spacing) with increasing plastic strain.

In order to deconvolute the hardness of the shear bands from that of the undeformed glass, we need a model for the composite hardness. We note that the softening associated with decreased shear-band spacing is reminiscent of the inverse Hall-Petch behavior in nanocrystalline materials below a critical grain [21,22]. The inverse behavior (strength decreasing with grain size) has been attributed to plastic deformation becoming hard within the crystalline grains but easy within the grain boundaries. In an analogous manner, we assume here that the deformed BMG consists of amorphous "grains," which are relatively hard, surrounded by soft shear-band "boundaries," which is reasonable given the gridlike pattern of the shear bands [Fig. 2(a)]. The stress to shear such a composite along a plane is given by [23]

$$\sigma = V_g \sigma_g + V_{sb} \sigma_{sb}, \quad (2)$$

where V_g is the fraction of undeformed glass on the shear plane, $V_{sb} = 1 - V_g$ is the shear-band fraction, and σ_g and σ_{sb} are the flow stresses of the undeformed glass and shear bands, respectively. Since hardness is proportional to flow stress, and $V_{sb} = t/d$, where t and d are the thickness and

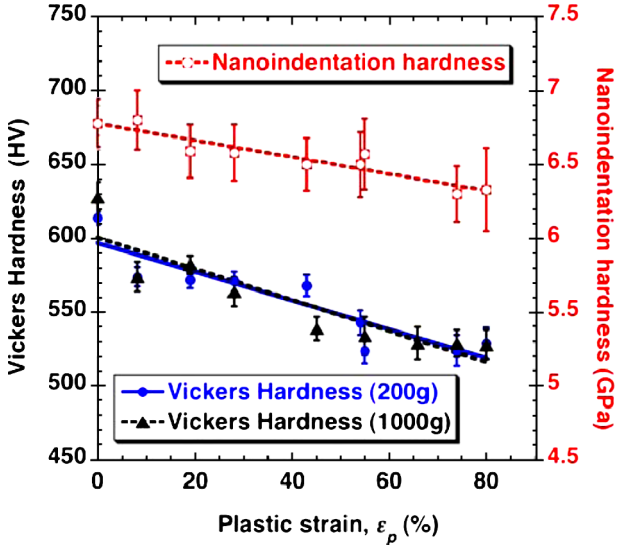

FIG. 3 (color online). Decrease in hardness (nanoindentation and Vickers at two different loads) with increasing plastic strain.

spacing, respectively, of the preexisting shear bands (which are intersected by the indentation shear bands), we obtain the following expression for the hardness of the deformed glass:

$$H = H_g - t(H_g - H_{sb})d^{-1}, \quad (3)$$

where H_g and H_{sb} are the hardnesses of the undeformed glass and the shear bands, respectively. Therefore, if H is plotted as a function of d^{-1}, as in Fig. 3, the intercept and slope of the linear fit yield values for H_g and $t(H_g\text{-}H_{sb})$, respectively. Recently, Lewandowski and Greer [24] showed that the shear-band thickness is on the order of 200–1000 nm. Using a middle value of 600 nm for the effective shear-band thickness t, we estimate from the nanoindentation data that $H_{sb} = 1.4$ GPa, which is considerably lower than the hardness of the undeformed glass $H_g = 6.7$ GPa. As a result of this lower hardness, plasticity, rather than spreading throughout the material, will tend to stay localized in a few shear bands, leading to the commonly observed shear instability and brittle fracture of metallic glasses.

In order to investigate possible mechanisms for this softening, we measured the thermal and elastic properties of the deformed glass. As demonstrated by the differential scanning calorimeter results in Fig. 4(b), a small decrease in the crystallization temperature with increasing strain was observed (~4 °C at $\varepsilon_p = 80\%$). It appears, therefore, that a portion of the work done during deformation remains stored in the BMG, perhaps as strain-induced local dilatation (increase in certain interatomic distances or the so-called free volume) [25]. A modest decrease in the Young's modulus with increasing strain (1%–2% decrease at $\varepsilon_p = 80\%$) was also observed [Fig. 4(a)], which is in agreement with Chen's earlier results [26]. The above results are

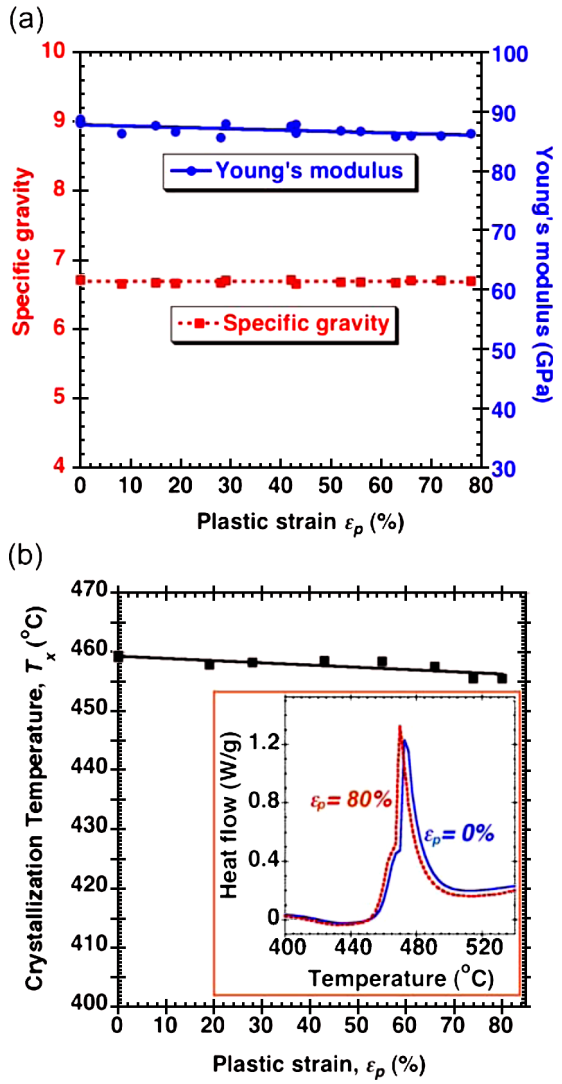

FIG. 4 (color online). (a) Young's modulus decreases slightly with increasing plastic strain, but specific gravity remains unchanged. (b) Crystallization temperature decreases slightly with increasing plastic strain.

consistent with a shear-induced local dilatation, which may be the source of the observed deformation-induced softening. Sometimes, this dilatation is manifested as a decrease in the specimen density [27], but in this study we did not observe such a change [Fig. 4(a)], either because our density measurements were not sensitive enough or because the dilation was highly localized in the shear bands and not detectable in an ''average'' measurement. Others have performed microstructural analysis of plastically deformed BMGs and shown that there is, indeed, an increase in free volume relative to the undeformed glass [28–32].

This research was sponsored by the Division of Materials Sciences and Engineering, Office of Basic Energy Sciences, U.S. Department of Energy under Contract No. DE-AC05-00OR22725 with UT-Battelle, LLC.

[1] R. W. Cahn, Nature (London) **341**, 183 (1989).
[2] A. L. Greer, Science **267**, 1947 (1995).
[3] P. Chaudhari and D. Turnbull, Science **199**, 11 (1978).
[4] W. L. Johnson, MRS Bull. **24**, 42 (1999).
[5] A. Inoue, Acta Mater. **48**, 279 (2000).
[6] G. E. Dieter, *Mechanical Metallurgy* (McGraw-Hill, New York, 1986).
[7] H. Bei, Z. P. Lu, and E. P. George, Phys. Rev. Lett. **93**, 125504 (2004).
[8] G. J. Shiflet, Y. He, and S. J. Poon, J. Appl. Phys. **64**, 6863 (1988).
[9] C. T. Liu *et al.*, Metall. Mater. Trans. A **29**, 1811 (1998).
[10] J. Schroers and W. L. Johnson, Phys. Rev. Lett. **93**, 255506 (2004).
[11] R. D. Conner, W. L. Johnson, N. E. Paton, and W. D. Nix, J. Appl. Phys. **94**, 904 (2003).
[12] R. D. Conner, Y. Li, W. D. Nix, and W. L. Johnson, Acta Mater. **52**, 2429 (2004).
[13] C. A. Schuh and T. G. Nieh, Acta Mater. **51**, 87 (2003).
[14] L. Q. Xing, Y. Li, K. T. Ramesh, J. Li, and T. C. Hufnagel, Phys. Rev. B **64**, 180201 (2001).
[15] T. Masumoto and R. Maddin, Mater. Sci. Eng. A **19**, 1 (1975).
[16] C. Tang, Y. Li, and K. Zeng, Mater. Sci. Eng. A **384**, 215 (2004).
[17] W. H. Jiang, F. E. Pinkerton, and M. Atzmon, Acta Mater. **53**, 3469 (2005).
[18] J. Lu, G. Ravichandran, and W. L. Johnson, Acta Mater. **51**, 3429 (2003).
[19] H. Kato, Y. Kawamura, A. Inoue, and H. S. Chen, Appl. Phys. Lett. **73**, 3665 (1998).
[20] A. Reger-Leonhard, M. Heilmaier, and J. Eckert, Scr. Mater. **43**, 459 (2000).
[21] J. Schiotz, F. D. Di Tolla, and K. W. Jachobsen, Nature (London) **391**, 561 (1998).
[22] H. Hahn, P. Mondal, and K. A. Padmanabhan, Nanostruct. Mater. **9**, 603 (1997).
[23] S. Takeuchi, Scr. Mater. **44**, 1483 (2001).
[24] J. J. Lewandowski and A. L. Greer, Nat. Mater. **5**, 15 (2006).
[25] F. Spaepen, Acta Metall. **25**, 407 (1977).
[26] H. S. Chen, Scr. Metall. **9**, 787 (1975).
[27] R. W. Cahn, N. A. Pratten, M. G. Scott, H. R. Sinning, and L. Leonardsson, in *Rapidly Solidified Metastable Materials*, edited by B. K. Kear and B. C. Giessen (Elsevier, New York, 1984), pp. 241–252.
[28] P. S. Steif, F. Spaepen, and J. W. Hutchinson, Acta Metall. **30**, 447 (1982).
[29] B. P. Kanungo, S. C. Glade, P. Asoka-Kumar, and K. M. Flores, Intermetallics **12**, 1073 (2004).
[30] K. M. Flores *et al.*, J. Mater. Res. **17**, 1153 (2002).
[31] J. Li, Z. L. Wang, and T. C. Hufnagel, Phys. Rev. B **65**, 144201 (2002).
[32] J. Li, F. Spaepen, and T. C. Hufnagel, Philos. Mag. A **82**, 2623 (2002).